Anal. Chem. **2001,** *73,* 5220−5227

Use of Gold Nanoparticles To Enhance Capillary Electrophoresis

Bela Neiman, Eli Grushka,* and Ovadia Lev*

Department of Analytical and Inorganic Chemistry, The Institute of Chemistry, and Division of Environmental Sciences, Fredy and Nadine Herrmann Graduate School of Applied Science, The Hebrew University of Jerusalem, Jerusalem, 91904 Israel

We describe here the use of gold nanoparticles to manipulate the selectivity between solutes in capillary electrophoresis. Two different gold-based nanoparticles were added to the run buffer. In one case, the nanoparticles were stabilized with citrate ions, but in another study, the gold nanoparticles were capped with mercaptopropionate ions (thiol-stablized). Citrate-stabilized gold nanoparticles were used in conjunction with capillaries treated with poly(diallyldimethylammonium chloride) (PDADMAC). The positively charged PDADMAC layer on the capillary walls adsorbs the negatively charged gold nanoparticles. The model solutes that were used to study the effect of the presence of the citrate-stabilized gold nanoparticles are structural isomers of aromatic acids and bases. The presence of the PDADMAC layer and the PDADMAC plus the gold nanoparticles changes both the electroosmotic mobility and the observed mobility of the solutes. These changes in the mobilities influence the observed selectivities and the separations of the system. Thiol-stabilized gold nanoparticles were used without PDADMAC in the capillary. The model solutes studied in this part are various aromatic amines. In this case as well, the presence of the gold nanoparticles modifies the electroosmotic mobility and the observed mobility of the solutes. These changes in the mobilities are manifested in selectivity alterations. The largest change in the selectivities occurs at low concentrations of the gold nanoparticles in the run buffer. The presence of nanoparticles improves the precision of the analysis and increases the separation efficiency.

Nanodispersions have attracted extensive attention in various fields of physics, biology, and chemistry.[1−5] Physicists and chemists are intrigued by the gradual transition of the nanomaterial properties from molecule-like to those of solid-state properties by a change of a single variable, the particle size. This property has practical and future applications for nonlinear optics and electronics. The large surface area of nanomaterials intrigues chemical engineers and catalysis scientists. Surprisingly, very little research has been devoted to the application of nanoparticles for chemical separation. In this work, we demonstrate the utility and versatility of organically modified gold nanoparticles in capillary electrophoresis (CE) separations. The nanoparticles serve as large surface area platforms for organofunctional groups that interact with the capillary surface, the analytes, or both. Thus, the apparent mobilities of target analytes, as well as the electroosmotic flow, can be altered leading to enhanced selectivities. Separation of various benzene derivatives demonstrates these capabilities.

Metallic nanodispersions can be prepared in aqueous and organic solvents using diverse procedures.[1,2,6−9] Nanodispersions can be stabilized in organic solvents by the solvent itself,[10] by the addition of long chain surfactants,[11,12] or by specific ligands.[13] Stabilization of metal nanodispersions in aqueous solutions is somewhat more complicated. Several successful stabilization methods are available that are based on capping of the metal nanoparticles (e.g., citrate,[6] 3-mercaptopropionate,[14] coenzyme A,[15] tiopronin,[15,16] glutathione,[17] 4-hydroxytiophenol[18]), by steric stabilization by polyelectrolytes [e.g., poly(vinylpyrrolidine), poly(ethylenoxide)][19,20] or by formation of stable silicate shell around the particles.[21,22]

* E-mail: Eli_Grushka@huji.ac.il and Ovadia@vms.huji.ac.il.

(1) Bradley, J. S. *Clusters and Colloids*; Schmid, G., Ed.; VCH: Weinheim, 1994; pp 459−554.
(2) Schmid, G. *Chem. Rev.* **1992**, *92*, 1709.
(3) Martin, C. R.; Mitchell, D. T. *Anal. Chem.* **1998**, *70*, 322A.
(4) Margel, S.; Burdygin, I.; Reznikov, V.; Nitzan, B.; Melamed, O.; Kedem, M.; Gura, S.; Mandel, G.; Zuberi, M.; Boguslavsky, L. *Recent Res. Dev. Polym. Sci.* **1997**, *1*, 51.
(5) Godovsky, D. Y. *Adv. Polym. Sci.* **2000**, *153*, 163.
(6) Grabar, K. C.; Freeman, R. G.; Hommer, M. B.; Natan, M. J. *Anal. Chem.* **1995**, *67*, 735.
(7) Yee, C. K.; Jordan, R.; Ulman, A.; White, H.; King, A.; Rafailovich, M.; Sokolov, J. *Langmuir* **1999**, *15*, 3486.
(8) Cheong Chan, Y. N.; Schrock, R. R.; Cohen, E. R. *Chem. Mater.* **1992**, *4*, 24.
(9) Ishizuki, N.; Torigoe, K.; Esumi, K.; Meguro, K. *Colloids Surf.* **1991**, *55*, 15.
(10) Fink, J.; Kiely, C. J.; Bethell, D.; Schiffrin, D. J. *Chem. Mater.* **1998**, *10*, 922.
(11) Johnson, S. R.; Evans, S. D.; Brydson, R. *Langmuir* **1998**, *14*, 6639.
(12) Torigoe, K.; Esumi, K. *Langmuir* **1992**, *8*, 59.
(13) Schmid, G.; Lehnert, A. *Angew. Chem., Int. Ed. Engl.* **1989**, *28*, 780.
(14) Yonezawa, T.; Sutoh, M.; Kunitake, T. *Chem. Lett.* **1997**, 619.
(15) Templeton, A. C.; Chen, S.; Gross, S. M.; Murray, R. W. *Langmuir* **1999**, *15*, 66.
(16) Templeton, A. C.; Cliffel, D. E.; Murray, R. W. *J. Am. Chem. Soc.* **1999**, *121*, 7081.
(17) Schaaff, T. G.; Knight, G.; Shafigullin, M. N.; Borkman, R. F.; Whetten, R. L. *J. Phys. Chem. B* **1998**, *102*, 10643.
(18) Chen, S. *Langmuir* **1999**, *15*, 7551.
(19) Mayer, A. B. R.; Mark, J. E. *Eur. Polym. J.* **1998**, *34*, 103.
(20) Mayer, A. B. R.; Johnson, R. W.; Hausner, S. H.; Mark, J. E. *J. Macromol. Sci., Pure Appl. Chem.* **1999**, *A36*, 1427.
(21) Liz-Marzán, L. M.; Giersig, M.; Mulvaney, P. *Langmuir* **1996**, *12*, 4329.
(22) Bharathi, S.; Fishelson, N.; Lev, O. *Langmuir* **1998**, *15*, 1929.

10.1021/ac0104375 CCC: $20.00
Published on Web 10/05/2001

In this paper, aqueous gold colloidal dispersions were prepared by the well-known citrate method that relies on reduction of $AuCl_4^-$ by citrate ions.[6] In one preparation, the citrate ions were used to stabilize the nanodispersion. In another procedure, citrate was used as a reductant and sodium 3-mercaptopropionate, as a stabilizer.[14]

Huber and co-workers,[23,24] as well as Rodriguez and Colon,[25,26] used polymer-based nanoparticles to coat fused silica capillaries for use in CE. Fujimoto and Muranaka[27] used commercially available silica gel nanoparticles as run buffer additive in CE. As far as we know, there has been no prior reported effort to use stabilized metal nanoparticles for capillary electrophoresis separation. We describe here a CE method using colloidal gold nanoparticles dispersed in the run buffer for capillary electrophoretic separations. Nanoparticle enhanced capillary electrophoresis can be thought of as pseudocapillary electrochromatography in which the nanoparticles play the role of the stationary phase. In addition, the interaction of the nanoparticles with the capillary wall can alter the electroosmotic velocity and even change its direction.

The use of nanoparticles as run buffer additives is similar to the use of micelle additives in micellar electrokinetic chromatography (MEKC).[28−30] In both cases, the purpose of the additive is to provide additional interaction sites with which the solutes can interact.

Both MEKC and nanoparticle-mediated capillary electrophoresis (NPCE) offer some definite advantages: (1) The presence of nanoparticles and micelles in the run buffer avoids the need to pack the capillary with a stationary phase. (2) Since there is no conventional stationary phase, the need for frits and other retaining techniques is eliminated. (3) Micelles and nanoparticles in the run buffer move through the capillary with an apparent mobility that takes into account the effects of both the electroosmotic flow (EOF) and their own native electrophoretic mobility. As a result, there is a constant turnover in the interacting media. The solutes are moving under the influence of electric field and are separated on the basis of their different effective charges and also by differential partitioning between the aqueous buffer and the nanoparticle or micellar pseudostationary phase. This additional partitioning effect increases the separation degrees of freedom and allows the separation not only of charged solutes but also of neutral ones. Thus, the user can control the nature of the interactions with the additives and tailor the CE system to specific analytes.

Although the use of nanoparticles and micelles in CE has a great many similarities, there are also some important differences between these two additives. One main difference between MEKC and NPCE is that in the former approach, the solutes can penetrate to the core of the micelles, whereas in the approach detailed here, the interactions with the solutes occur always at the outer surface of the nanoparticles. These interactions can be either with the surface itself or with the organic moieties attached to the surface of the nanoparticle.

Additionally, NPCE extends the operable range to much higher fields. The operable field in CE is limited to a large extent by thermal effects induced by the applied voltage and by the generated current. Therefore, it is advantageous whenever possible to operate the CE at low ionic strength. In the case of MEKC, it is necessary to use high surfactant concentration that exceeds the CMC. Stabilized nanoparticles do not suffer from this drawback, and stable colloidal solutions are attained even with no dissolved species.

The aim of the present paper is to demonstrate that the presence of gold nanoparticles in the run buffer has the ability to affect significantly the apparent mobilities of certain solutes as well as to change the electroosmotic mobility of the run buffer. The change in apparent and electroosmotic mobilities alter significantly the migration times of the solutes, the selectivities between them, and their peaks' shape. We also demonstrate that both run-to-run reproducibility and separation efficiency improve by the introduction of gold nanoparticles to the run buffer.

MATERIALS AND METHODS

Capillary Electrophoresis. Analyses were performed on a Bio-Rad BioFocus 2000 capillary electrophoresis system using a UV detector operated at 254 nm. Polyimide-coated fused-silica capillaries, 50 μm i.d., 375 μm o.d. (Polymicro, CA), were employed in the study. The capillary total length was 26.8 cm. The effective length (from injection point to detector) was 22 cm. Samples were injected hydrodynamically by applying 5.0 psi head pressure for 0.4 s. Electrophoretic separations were performed at applied voltages of 10 kV. Between the runs, the capillary was washed sequentially with sodium hydroxide, water, and run buffer, each for a 1-min period. Modified capillaries were washed between runs with only the run buffer for 1.5 min. Data were recorded on a PC.

Chemicals and Standards. Aminophenols were obtained from Eastman Organic Chemicals, N.Y.; toluidines were from Merck (Germany); toluic acids, hydroxybenzoic acids, phenylendiamines, and anisidines were purchased from Aldrich, Israel.

When using citrate-stabilized nanoparticles, aminophenols and toluidines were dissolved in the run buffer at concentrations of 10^{-3} M. Toluic acids and hydroxybenzoic acids were dissolved at concentrations of 2×10^{-3} M. The run buffer used with the citrate-stabilized gold nanoparticles was prepared by mixing 0.02 M sodium acetate solution (Merck, Germany) and 0.02 M acetic acid (Frutarom, Israel) at a 70:30 volume ratio. The final pH of the buffer was 5.

In the studies using 3-mercaptopropionate (thiol)-stabilized gold nanoparticles, all of the solutes were dissolved at concentrations of 2×10^{-3} M. The run buffer used with the thiol-stabilized gold nanoparticles was prepared by adjusting the pH of a 0.005 M sodium phosphate dibasic heptahydrate solution (Aldrich, Israel) to 6.4 with concentrated (15 M) phosphoric acid (Baker, Holland).

The preparation of the buffers and samples used TDW water. Buffers and sample solutions were filtered through 0.45-μm syringe filters. In some of the studies, poly(diallyldimethylammo-

(23) Kleindienst, G.; Huber, C. G.; Gjerde, D. T.; Yengoyan, L.; Bonn, G. K. *Electrophoresis* **1998**, *19*, 262.
(24) Huber, C. G.; Premstaller, A.; Kleindienst, G. *J. Chromatogr. A.* **1999**, *849*, 175.
(25) Rodriguez, S. A.; Colon, L. A. *Anal. Chim. Acta* **1999**, *397*, 207.
(26) Rodriguez, S. A.; Colon, L. A. *Chem. Mater.* **1999**, *11*, 754.
(27) Fujimoto, C.; Muranaka, Y. J. *High Resolut. Chromatogr.* **1997**, *20*, 400.
(28) Terabe, S.; Otsuka, K.; Ichikawa, K.; Tsuchiya, A.; Ando, T. *Anal. Chem.* **1984**, *56*, 111.
(29) Terabe, S. *Capillary Electrophoresis Technology*; Guzman, N. A., Ed.; Marcel Dekker: New York, 1993.
(30) Shamsi, S. A.; Palmer, C. P.; Warner, I. M. *Anal. Chem.* **2001**, *73*, 140A.

nium) chloride (PDADMAC) was used to modify the inner surface of the capillary. For that purpose we used PDADMAC (Hoechst, Germany) with molecular weight of about 120 000. A 0.05-g portion of PDADMAC was dissolved in 25 mL of buffer (1:500 dilution), and this solution was used for surface modification.

Hydrogen tetrachloroaurate(III) trihydrate was obtained from Aldrich, Israel, and sodium citrate dihydrate was obtained from Mallinckrodt, France. 3-Mercaptopropionic acid was purchased from Aldrich, Israel. Sodium hydroxide was obtained from Frutarom (Israel).

Mesityl oxide (Aldrich, Israel) was used as the neutral electroosmotic flow marker.

Gold Nanoparticles Preparation. Citrate-stabilized gold nanoparticles were prepared according to the Grabar procedure.[6] Using transmittance electron microscopy (TEM) the nanoparticles were found to have an average diameter of 18 nm. The initial concentration of the hydrogen tetrachloroaurate(III) trihydrate, used to prepare the nanoparticles, was 0.25 mM.

Sodium 3-mercaptopropionate gold nanoparticles were prepared according to the Yonezawa procedure.[14] The size of gold nanoparticles is controlled by the gold/stabilizer ratio. In our work, that ratio was chosen as 1.0. TEM measurements showed that the average size of the thiol-stabilized nanoparticles was ~5 nm. The initial concentration of the hydrogen tetrachloroaurate(III) trihydrate used to prepare the nanoparticles was about 0.73 mM.

Initial Capillary Treatment. A 50-μm i.d. fused-silica capillary of desired length was mounted into the CE system and washed sequentially with 1 M sodium hydroxide for silanol activation (10 min), water (10 min), and buffer (5 min). After the washing stage, the run buffer solution was pumped through the capillary, and the high voltage (10 kV) was turned on for about an hour. At this stage, the capillary was ready for use in analysis.

Preparation of Particle-Coated Capillaries. A run buffer solution containing PDADMAC (in a 1:500 dilution of the original PDADMAC material) was pumped through the capillary for 30 min without voltage operation. After the polymer adsorption, the capillary was flushed for 10 min with the acetate run buffer solution containing PDADMAC at 1:5000 dilution. The modified capillary was then characterized electrophoretically by injecting the appropriate solutes using acetate buffer. Next, the citrate-stabilized gold nanoparticle solution was pumped through the capillary for 30 min. Electrophoretic parameters were then measured using run buffer containing different concentrations of gold nanoparticles.

RESULTS AND DISCUSSION

Estimation of the Nanoparticle Concentration. It is of importance to estimate the concentration of the nanoparticles and of the organic groups attached to them. From the size of the nanoparticles (18 nm for the citrate-stabilized and 5 nm for the thiol-stabilized nanoparticles) and the molar volume of gold (10.2 mL/mol) we can estimate the number of gold atoms in a single nanoparticle. Knowing the original concentrations of the gold solutions, and assuming 100% conversion to nanoparticles, we calculated the number of nanoparticles per liter. Using the conventional definition of the mole we calculated the initial concentration of the nanoparticles in the reaction vessel. With the citrate-stabilized nanoparticles, the concentration is estimated to be 1.4 nM, but in the case of the thiol-stabilized nanoparticles, the concentration is estimated to be 0.19 μM. These solutions were diluted as needed for the experiments. The concentration values in the discussion that follows are the diluted values.

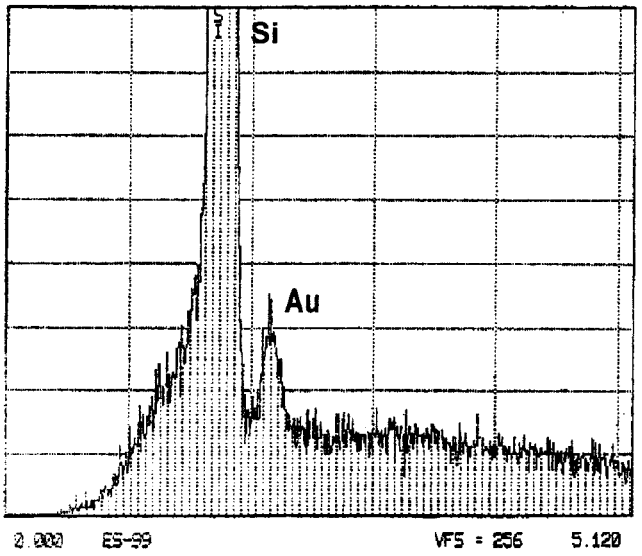

Figure 1. Graphic energy-dispersive X-ray of capillary inner surface.

Characterization of PDADMAC-Coated Capillaries. The citrate- and the mercaptopropionate-capped gold nanoparticles form stable sols. No visual signs of decomposition or precipitation were observed over a period of several months. The UV−vis spectra of all gold nanoparticle solutions prepared by us showed the typical surface plasmon absorption around 520 nm.

In the studies with adsorbed PDADMAC, it is reasonable to assume that the negatively charged citrate-stabilized gold nanoparticles will be adsorbed on the positively charged capillary wall. To verify the adsorption of the citrate-stabilized gold nanoparticles, an electron probe microanalyzer (EPMA) was used. After passing the gold nanoparticles solution through the PDADMAC treated capillary, the capillary was removed from its cartridge and cut diagonally with a razor blade. SEM images (not shown) confirmed the presence of gold nanoparticles.

Energy dispersive X-ray fluorescence (EDXRF) (Figure 1) showed a characteristic gold peak (1.74 keV) in addition to the expected silicon peak (2.12 keV). For comparison, we also used EDXRF to examine the outer wall of the capillary underneath the polyimide coating. As anticipated, no gold signal was found on the outer wall.

Although electron microscopy corroborated the presence of gold on the inner wall of the capillary, the exact amount of the adsorbed gold nanoparticles is not known at this stage. Neither do we know if the gold nanoparticles are in the form of a monolayer or a several-layer deposit.

Separations in Gold-Modified Capillaries. *Separations in Citrate-Stabilized Gold-Coated Capillaries.* With nontreated capillaries, the electroosmotic flow (EOF) was in the cathodic direction. It should be noted that mesityl oxide was used as a neutral marker in these studies. Although it is possible that mesityl oxide can have some interactions with other components in the run buffer (primarily the gold nanoparticles), we did not see any evidence for such interactions. The negatively charged fused-silica walls determine the cathodic direction of the EOF. Using untreated capillaries, positive solutes, such as aminophenols and toluidines,

Table 1. Electroosmotic Mobilities in a New Capillary after PDADMAC Coating and after Treatment with Citrate-Stabilized Gold Nanoparticles

concn gold nanoparticles (nM)	electroosmotic mobility ($\times 10^{-4}$) ($cm^2\ V^{-1}\ sec^{-1}$)
0 (new capillary)	2.82
0 (capillary treated with PDADMAC only)	−6.920
0.014	1.58
0.14	1.59
0.28	2.05
0.42	2.58

migrated toward the cathode, and they emerged from the capillary before the EOF marker. Negative solutes, such as toluic acids and hydroxybenzoic acids, migrated to the anode. The electrophoretic mobilities of the negatively charged solutes studied here were greater (in absolute terms) than the electroosmotic mobility. Thus, the voltage polarity had to be reversed for these solutes to reach the detector. At the pH of these studies, the negatively charged solutes, although exhibiting reasonable within-run precision (relative standard deviation of 3−5%), had shown poor between-run reproducibility. The reason for the poor reproducibility of the negatively charged solutes is the proximity of the pH to the pK_a of the solutes. Positively charged solutes as well as the neutral marker (mesityl oxide) showed much better precision and reproducibility, typically between 1 and 2% relative standard deviation.

Modification of the capillary wall with PDADMAC covers the silanol groups with positive quaternary ammonium groups to produce a much more homogeneous wall surface. As a result of the positive wall, the EOF changes its direction from cathodic to anodic. The absolute value of the EOF changes, as well. Table 1 shows the EOF values for the various conditions used in this study.

With the PDADMAC modification but without the gold nanoparticles in the run buffer, the toluidines, the aminophenols, and the toluic acids migrate toward the anode. The positively charged solutes migrate slower than the EOF, and the negatively charged solutes migrate faster than the EOF. The more homogeneous layer of PDADMAC on the capillary inner wall stabilizes the electroosmotic flow, giving more reproducible migration data. For both negatively and positively charged solutes, the precision in the migration data is 1−1.5%. Additionally, PDADMAC-modified capillaries yield more efficient separations with more symmetrical peaks.

Passing the citrate-stabilized gold solution through the PDADMAC-modified capillary resulted in the electrostatic adsorption of the negatively charged nanoparticles on the positively charged walls. Since the adsorbed layer of the citrate-stabilized gold nanoparticles is negatively charged, the EOF reverses its direction again toward the cathode (see Table 1). The absolute magnitude of the electroosmotic mobility is decreased significantly relative to the mobility in the PDADMAC-treated capillary. As shown in Table 1, each additional increase in the gold concentration caused an additional small rise in the electroosmotic mobility. Increasing the amount of the gold nanoparticles in the run buffer by a factor of 30 changed the electroosmotic flow by less than a factor of 2. The results indicate that the low concentration of the gold

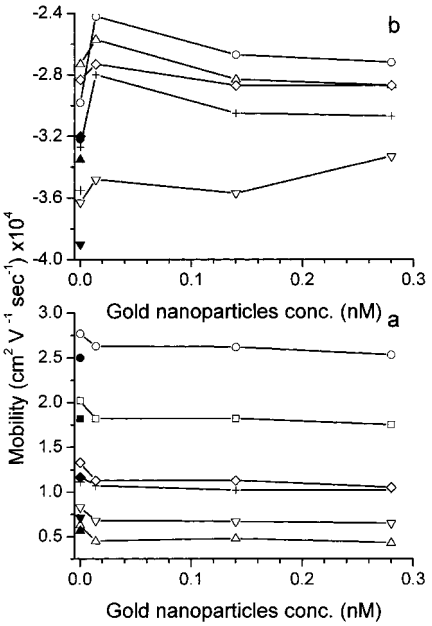

Figure 2. Dependence of the apparent mobilities on the concentration of citrate-stabilized gold nanoparticles in the run buffer. The solid symbols indicate electrophoretic mobilities obtained on new untreated capillaries. (a) Positively charged solutes: ○, *p*-aminophenol; □, *p*-toluidine; ◇, *m*-toluidine; +, *o*-aminophenol; ▽, *o*-toluidine; △, *m*-aminophenol. (b) Negatively charged solutes: △, *m*-toluic acid; ◇, *m*-hydroxybenzoic acid; ○, *p*-toluic acid; +, *o*-toluic acid; ▽, *o*-hydroxybenzoic acid. In the case of negatively charged solutes, the polarity of the electric filed was adjusted so that the detector was on the anodic side. In the case of positively charged solutes, the detector was on the cathodic side, except when the PDADMAC-treated capillary was used.

nanoparticles is sufficient to provide enough nanoparticles to occupy the great majority of the available adsorption sites on the PDADMAC layer. Any additional increase in the concentration of the gold particle in the run buffer does not contribute significantly to the number of nanoparticles adsorbed on the PDADMAC.

Before discussing the effect of the gold nanoparticles on the behavior of the solutes, we need to define some mobility terms. The electrophoretic mobility, μ_{ef}, is the mobility of the solute in the neat run buffer under the influence of an electric field. In the presence of PDADMAC or gold nanoparticles in the run buffer, the migration of the solute can be modified by interactions with the additive in the buffer. The mobility in this case will be termed apparent mobility, μ_{ap}. The observed mobility, μ_{obs}, signifies the mobility calculated from the experimental migration time, and it takes into account the electroosmotic flow, as well.

The adsorption of PDADMAC on the capillary and the subsequent introduction of the citrate-stabilized gold nanoparticles all change the apparent mobilities. The extent of the change depends on the charge of the solutes and their functional group(s). Moreover, the change in μ_{ap} is often different for structural isomers of the same group. Figure 2 depicts the dependence of the apparent mobilities on the concentration of the citrate-stabilized nanoparticles. Figure 2a shows the behavior of positively charged solutes, and Figure 2b is for the negatively charged solutes. Each panel contains a set of open markers connected by a line and a set of solid (filled) single-point markers on the *y*-axis.

The connected open markers depict the behavior of μ_{ap} as a function of the nanoparticles concentration, starting at a PDADMAC-modified capillary without any nanoparticles. The solid symbols give the data obtained from a new capillary before treatment with PDADMAC and the introduction of gold nanoparticles. Open and solid symbols of the same shape represent the same solute.

From Figure 2a, we see that for the positive solutes, the apparent mobilities obtained on PDADMAC-modified capillaries (before the introduction of the gold nanoparticles) are larger than the mobilities obtained on new capillaries. The order of the migration is in line with the degree of ionization of the solutes: the higher the degree of ionization, the larger is the apparent mobility. Upon the introduction of the citrate-stabilized gold nanoparticles, the apparent mobility of the positively charged solutes decreases. A further increase in the number of gold nanoparticles causes very little change in the magnitude of the apparent mobilities. The initial drop in the μ_{ap} values can be explained in terms of the attraction of the amine groups to the gold nanoparticles, resulting in a decrease in the effective charge of the solutes.

With the negatively charged solutes (Figure 2b), the introduction of PDADMAC decreases the absolute value of the apparent mobilities. The introduction of the citrate-stabilized gold nanoparticles to the run buffer resulted in a further decrease in the apparent mobility of the solutes. Increasing the concentration of the nanoparticles in the buffer caused little change to the μ_{ap} values.

The electrophoretic selectivity, α, is defined here as the ratio of the electrophoretic mobilities of two neighboring solutes in the electropherogram.

$$\alpha_{ef} = \frac{\mu_{ef,2}}{\mu_{ef,1}} \tag{1}$$

The index 1 and 2 identifies the solutes. Similarly, the apparent selectivity, α_{ap}, is the ratio of two neighboring apparent mobilities.

$$\alpha_{ap} = \frac{\mu_{ap,2}}{\mu_{ap,1}} \tag{2}$$

The addition of PDADMAC to the capillary causes relatively small change in the α_{ap} values; compare the "new capillary" column in Table 2 with the zero Au concentration column. The initial introduction of the gold nanoparticles yields the greatest change in the apparent selectivity. Further increase in the concentration of the nanoparticles has minimal effect on α_{ap}. The data in Table 2 shows that for positively charged solutes, the introduction of gold nanoparticles increases the apparent selectivity, but with the negatively charged solutes, α_{ap} decreases.

In the presence of electroosmotic flow, the observed selectivity, α_{obs}, can be substantially different from the electrophoretic or apparent selectivity. The EOF vector can either enhance or diminish the electrophoretic or apparent selectivity. The observed selectivity is described by

$$\alpha_{obs} = \frac{t_{m,2}}{t_{m,1}} = \frac{\mu_{obs,2}}{\mu_{obs,1}} = \frac{\mu_{ap,2} + \mu_{eo}}{\mu_{ap,1} + \mu_{eo}} \tag{3}$$

Table 2. Dependence of the Apparent Selectivity on the Presence of PDADMAC and the Concentration of the Citrate-Stabilized Gold Nanoparticles[a]

		concn of Au nanoparticles (nM)			
	new cap.	0	0.014	0.14	0.28
p/*o*-aminophenol	2.24	2.34	2.47	2.57	2.49
o/*m*-aminophenol	1.97	1.87	2.37	2.10	2.35
p/*m*-toluidine	1.56	1.51	1.60	1.60	1.67
m/*o*-toluidine	1.63	1.60	1.66	1.70	1.62
o/*m*-toluic acid	1.06	1.20	1.09	1.08	1.07
m/*p*-toluic acid	1.04	0.92	1.06	1.06	1.06
o/*m*-hydroxybenzoic acid	1.22	1.28	1.27	1.24	1.16

[a] The column of 0 concentration of gold nanoparticles depicts the behavior in the PDADMAC-modified capillary.

Table 3. Dependence of the Observed Selectivity on the Presence of PDADMAC and the Concentration of the Citrate-Stabilized Gold Nanoparticles[a]

		Au concn (nM)			
	new cap.	0	0.014	0.14	0.28
EOM $\times 10^4$ cm^2/(V sec)	2.82	−6.92	1.58	1.59	2.05
p/*o*-aminophenol	1.35	0.72	1.59	1.61	1.49
o/*m*-aminophenol	1.16	0.91	1.30	1.26	1.23
p/*m*-toluidine	1.16	0.88	1.25	1.25	1.23
m/*o*-toluidine	1.13	0.92	1.20	1.21	1.15
o/*m*-toluic acid	1.38	1.06	1.24	1.17	1.24
m/*p*-toluic acid	1.34	0.97	1.18	1.15	1.23
o/*m*-hydroxybenzoic acid	2.84	1.08	1.65	1.61	1.86

[a] The column of 0 concentration of gold nanoparticles gives the behavior in the PDADMAC-modified capillary. Also given in the table are the electroosmotic mobilities for each of the conditions.

where t_m represents migration times and indexes 1 and 2 denote the solutes in question. The importance of the magnitude and direction of the electroosmotic mobility vis-à-vis the magnitude and direction of the apparent (or electrophoretic for that matter) mobility is discussed by Kenndler.[31]

Table 3 summarizes the effect of citrate-stabilized gold nanoparticles in the run buffer on the observed selectivities of several solutes. The electroosmotic mobility values under each working condition are also given in the table.

The observed selectivities in Table 3 behave as expected from eq 3. For the positively charged solutes, α_{obs} decreases slightly with increasing μ_{eo}. For the negatively charged solutes, since $|\mu_{eo}| < |\mu_{ap}|$,[31] the selectivities increase with increasing μ_{eo}. It should be noted that with the untreated capillary, the electroosmosis is the fastest and, as a consequence, the selectivities are also the highest.

Figure 3 shows the electropherograms obtained for the toluidines. Figure 3a was obtained with a new capillary, and Figure 3b is with a PDADMAC-modified capillary and a run buffer containing 0.014 nM gold nanoparticles. The effect of the gold nanoparticles on the observed behavior of the toluidines is evident: the migration times are longer, and the observed selectivities are greater. It should be stressed here that the main aim of the current research was to demonstrate that the presence

(31) Kenndler, E. *High Performance Capillary Electrophoresis*; Khaledi, M. G., Ed.; John Wiley and Sons, Inc.: New York, 1998, pp 25−76.

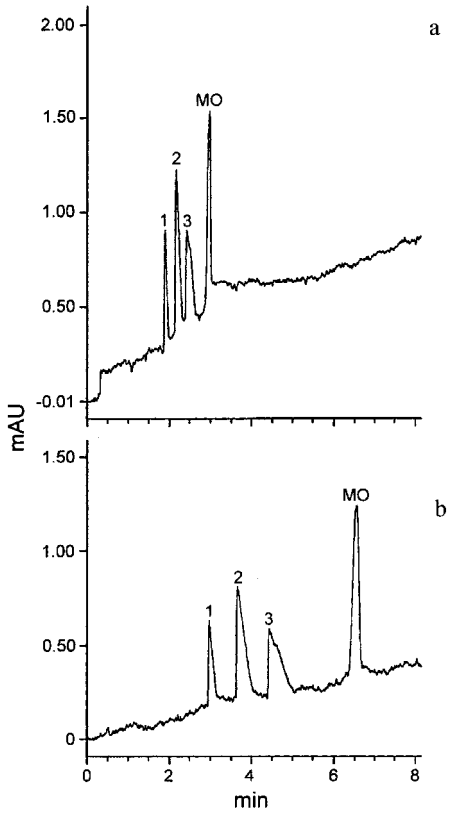

Figure 3. Electropherograms of toluidines in (a) fused-silica capillary without a modifier, (b) using a run buffer containing 0.014 nM gold nanoparticles with the PDADMAC modified capillary. The run buffer was pH 5, 0.02 M acetate buffer. Peak identification: (1) *p*-toluidine, (2) *m*-toluidine and (3) *o*-toluidine. MO stands for the EOF marker mesityl oxide. The detector was on the cathodic side of the capillary.

of gold nanoparticles affects the selectivity between the analytes. At the pH of the experiments (dictated by the gold nanoparticles synthesis), the toluidines isomers are well-separated, even on an unmodified capillary. The separation is better in the presence of the gold nanoparticles.

The observed precision obtained with the citrate-stabilized gold nanoparticles was much better than the precision in the case of the untreated capillary but less than the precision observed with the PDADMAC-treated capillary.

An attempt to use citrate-stabilized nanoparticles in the run buffer without PDADMAC in the capillary was unsuccessful. When we used gold nanoparticles at the same concentration level as with the PDADMAC, no effect was observed on the electrophoretic parameters. With higher nanoparticle concentrations, the run buffer solution was not stable, and with time, the nanoparticles precipitated out. In addition, the application of 10 kV fields caused the nanoparticles to precipitate.

Separations with 3-Mercaptopropionate-Gold-Modified Capillaries. Thiol-containing compounds are known to form stable covalent bonds with gold surfaces.[32] This strong interaction between thiol-containing compounds and gold surfaces allows us to prepare thiol-stabilized gold nanoparticles. The thiol that we used here was sodium 3-mercaptopropionate so that the nanoparticles were negatively charged. The thiol-stabilized gold nanoparticles solution

(32) Finklea, H. O. *Electroanalytical Chemistry*; Bard, A. J., Rubinstein, I., Eds.; Marcel Dekker, Inc.: New York, 1996; Vol. 19.

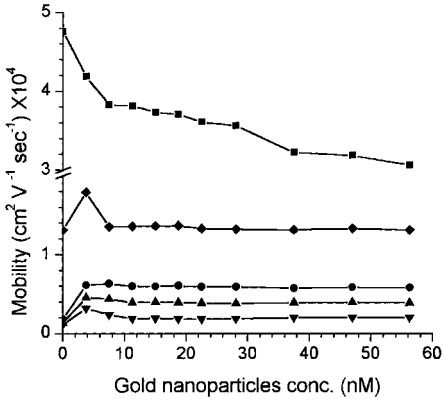

Figure 4. Dependence of the electroosmotic mobility and the apparent mobility on the concentration of the thiol-stabilized gold nanoparticles in the run buffer: ■, electroosmosis; ◆, *p*-phenylenediamine; ●, *p*-aminophenol; ▲, *p*-anisidine; ▼, *p*-toluidine. The detector was on the cathodic side of the capillary.

is quite robust and does not require the use of PDADMAC for additional stabilization. In all of the following experiments, PDADMAC was not preadsorbed onto the capillaries prior to the use of the thiol-stabilized gold nanoparticles.

In general, we found that negatively charged solutes gave asymmetric and broad peaks. As a result, we will discuss at present only the behavior of positively charged solutes.

As can be seen in Figure 4, the presence of the thiol-stabilized gold nanoparticles in the run buffer decreases noticeably the electroosmotic mobility. This decrease in μ_{eo} is different from the behavior observed with the citrate-stabilized gold nanoparticles in the PDADMAC-treated capillaries in which the μ_{eo} increased with increasing concentration of the nanoparticles. The decrease in μ_{eo} is related to changes in the ionic strength of the run buffer. The ionic strength of the phosphate run buffer used in this set of experiments is relatively low (0.012 M); therefore, increasing the concentration of the multi-charged nanoparticles in the run buffer increases significantly the total ionic strength of the buffer. It is well-established that as the ionic strength of the run buffer increases, the electroosmotic mobility decreases.[33,34]

The apparent mobilities show a different dependence on the concentration of the thiol-stabilized gold nanoparticles. As we see in Figure 4, the initial introduction of the nanoparticles increases substantially the apparent mobilities of the solutes studied here. Further increase in the concentration of the gold nanoparticles decreases slightly the apparent mobilities of the solutes. With the exception of *p*-phenylenediamine, the μ_{ap} values of the solutes at the highest nanoparticles concentration are still higher than the mobilities without nanoparticles in the run buffer. In the case of *p*-phenylenediamine, its apparent mobility increases initially but then μ_{ap} returns to the level obtained with the neat buffer.

For both the citrate-stabilized and thiol-stabilized nanoparticles, their initial introduction to the run buffer caused the largest change in the apparent mobilities of the solutes. In addition, in both cases, further increase in the concentration of the nanoparticles did not result in a large change of μ_{ap}. However, the direction

(33) Bruin, G. J. M.; Chang, J. P.; Kuhlman, R. H.; Zegres, K.; Kraak, J. C.; Poppe, H. *J. Chromatogr.* **1989**, *471*, 429.

(34) VanOrman, B. B.; Liversidge, G. G.; McIntire, G. l.; Olefirowich, T. M.; Ewing, A. G. *J. Microcolumn Sep.* **1990**, *2*, 176.

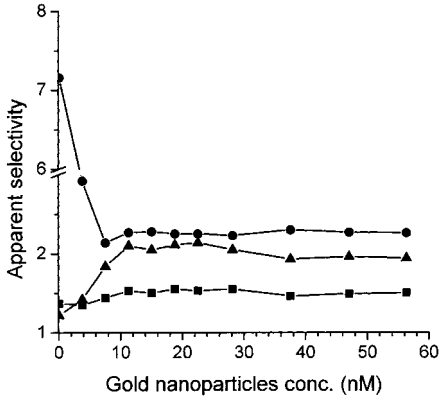

Figure 5. Apparent selectivity as a function of the thiol-stabilized gold nanoparticle concentration: ●, *p*-phenelynediamine/*p*-aminophenol; ▲, *p*-anisidine/*p*-toluidine; ■, *p*-aminophenol/*p*-anisidine.

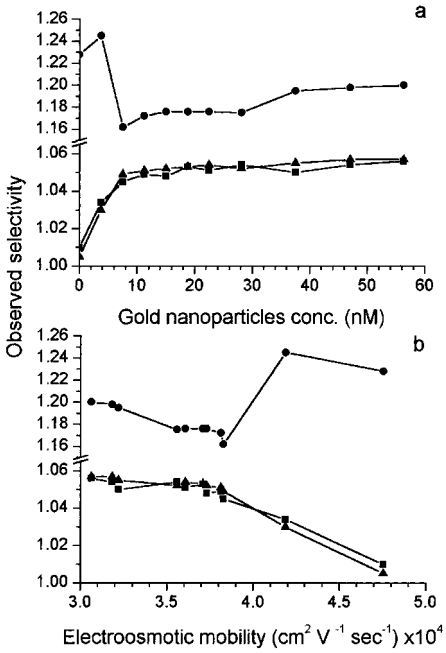

Figure 6. Observed selectivity versus (a) thiol-stabilized gold nanoparticle concentration and (b) electroosmotic mobility: ●, *p*-phenelynediamine/*p*-aminophenol; ▲, *p*-anisidine/*p*-toluidine; ■, *p*-aminophenol/*p*-anisidine.

of the changes in μ_{ap} is dependent on the type of nanoparticles. With the citrate-stabilized nanoparticles, the general trend was to lower the apparent mobilities, but with the thiol-stabilized nanoparticles, the trend is toward higher apparent mobilities.

As discussed above, the apparent mobilities of the various solutes were, to a large extent, independent of the amount of the nanoparticles (both citrate- and thiol-stabilized) at the higher concentration range of the nanoparticles. We attribute this independence to surface adsorption of the nanoparticles that occurs upon the first introduction of the nanoparticles to the capillary. The solutes are affected by the adsorption of the nanoparticles and, as a result, their apparent mobility changes. The initial introduction of the nanoparticles occupies the great majority of the available active sites on the capillary wall and, therefore, any further increase in the concentration of the gold nanoparticles in the run buffer does not add new interaction sites for the solute molecules. Figure 4 indicates that the interactions between the solutes and the nanoparticles in the buffer (not those adsorbed on the wall) are relatively weak.

The dependence of the apparent selectivities on the concentration of the thiol-stabilized gold nanoparticles is shown in Figure 5. As expected, the greatest change in α_{ap} occurs at low nanoparticle concentration (between 0 and 4 nM), because in this concentration region, the interactions between the solutes and the gold nanoparticles are the greatest. At the high end of the concentration scale (>4 nM), α_{ap} is independent of the amount of nanoparticles in the buffer. This independence in μ_{ap} is a direct result of the relatively constant mobilities at high nanoparticle concentrations.

As was the case for the citrate-stabilized gold nanoparticles, the observed selectivity, α_{obs}, which takes into account both the apparent and electroosmotic mobilities (see eq 3), is the important parameter from a separation point of view. Figure 6a shows α_{obs} as a function of the concentration of the thiol-stabilized gold nanoparticles. Figure 6b plots the dependence of α_{obs} on the electroosmotic mobility.

In Figure 6a, as in Figure 5, we can divide the behavior of the observed selectivity into two regions. At low nanoparticle concentrations (0−4 nM), where the extent of interaction between the solutes and the gold nanoparticles increases with increasing nanoparticles concentrations, the change in the observed selectivity is pronounced. Above 4 nM, any further increase in the concentration of the gold nanoparticles does not change the extent of solute−nanoparticle interactions, and the observed selectivity changes mainly as a result of the changes in the electroosmotic mobility. In fact, in Figure 6b, we see that at the high end of the μ_{eo} axis, corresponding to low concentrations of the thiol-stabilized gold nanoparticles, the dependence of the observed selectivity on the electroosmotic mobility deviates from the theoretically expected behavior,[31] where α_{obs} should rise very rapidly. However, at the lower part of the μ_{eo} axis (below about 3.75×10^{-4} cm^2 V^{-1} sec^{-1}, corresponding to nanoparticles concentration of above 4 nM) the observed selectivity changes much more in accordance to the predicted behavior of eq 3.

At the conditions of the analysis, in the absence of the thiol-stabilized gold nanoparticles, we could not separate *p*-anisidine from *p*-toluidine and *p*-aminophenol from *p*-anisidine. With the introduction of the gold nanoparticles, the observed selectivities increased sufficiently, as seen in Figure 6, so that the above two solute pairs can now be resolved. Figure 7a shows an electropherogram where, in the absence of gold nanoparticles, *p*-anisidine, *p*-toluidin,e and *p*-aminophenol comigrate with mesytil oxide. In Figure 7b, the separation of all of the solutes is accomplished with 75 nM gold nanoparticles in the run buffer.

In addition to selectivity improvement, the use of gold nanoparticles provides for some additional benefits. For example, the presence of the thiol-stabilized gold nanoparticles in the run buffer improves the precision of the collected data. Typical relative standard deviation values of the migration times are <0.5%. Without the gold nanoparticles, the relative standard deviation values are ∼2.3%. Similarly, the use of the gold nanoparticles improves the efficiency of the separation. For example, *N* increases from around 8600 obtained without gold in the run buffer to around 18 600 plates obtained with a run buffer containing 75 nM gold nanoparticles. We should point out that although in general,

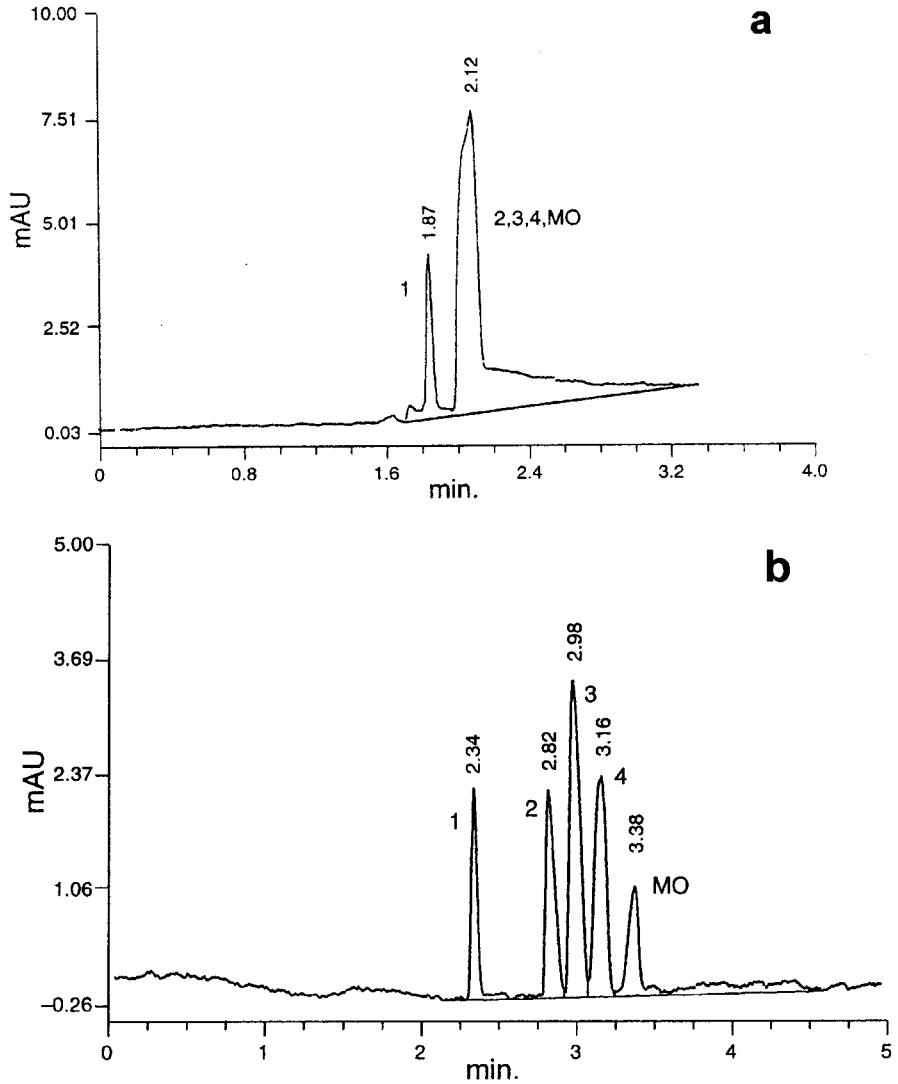

Figure 7. Electropherograms of (1) *p*-phenylendiamine, (2) *p*-aminophenol, (3) *p*-anisidine, and (4) *p*-toluidine (a) without gold nanoparticles in the run buffer and (b) with 75 nM 3-mercaptopropionate gold nanoparticles in the run buffer. The detector was on the cathodic side of the capillary.

both the citrate-stabilized and the thiol-stabilized nanoparticles gave more efficient and more reproducible CE separations, the thiol-stabilized nanoparticles resulted in better CE systems.

CONCLUSIONS

The presence of gold nanoparticles, whether citrate-stabilized or thiol-stabilized, changes the electroosmotic mobility as well as the observed mobilities of the solutes. The change in the observed mobilities is due to canges in the electroosmotic mobility of the buffer and the interaction between the solutes and the additives, such as PDADMAC and nanoparticles. The extent of these interactions is most pronounced when the concentration of the nanoparticles in the run buffer is less than that of the solutes. Above a certain concentration level, any further increase in the amount of nanoparticles in the run buffer changes the mobilities only slightly.

The changes in the mobilities, due to the presence of the gold nanoparticles in the run buffer, are manifested in changes in the selectivities. Both the apparent selectivities and the observed selectivities, which take into account the effect of the electroosmotic flow, are affected. The presence of the gold nanoparticles in the run buffer allows us to obtain separations that cannot be achieved without the nanoparticles. Additional benefits of using gold nanoparticles are improved precision in the data and improved efficiency, as expressed by the plate numbers.

ACKNOWLEDGMENT

This research was supported by Grant No. 1999199 from the United States−Israel Binational Science Foundation (BSF), Jerusalem, Israel.

Received for review April 16, 2001. Accepted August 8, 2001.

AC0104375